


Packages of Short-Period Internal Waves on the Black Sea Shelf Based on the Measurement Data of the Thermoresistor Chains Cluster

V. V. Ocherednik , A. G. Zatsepin

Shirshov Institute of Oceanology, Russian Academy of Sciences, Moscow, Russian Federation

 v.ocherednik@ocean.ru

Abstract

Purpose. The study is purposed at calculating and analyzing the characteristics of short-period internal wave (IW) packages based on the long-term measurements of vertical temperature distributions by a cluster of three moored thermoresistor chains spaced apart from each other and placed on the Black Sea shelf in the Golubaya Bay area (the Southern Branch of IO RAS, Gelendzhik).

Methods and Results. Measurements were carried out in 2018–2020. A cluster of three thermoresistor chains at the moored buoy stations supplied with the submerged buoys was located at a distance of about 1300 m from the coast and connected to a multi-modem station, through which the data was transmitted online to the onshore data server via a fiber optic cable. The moored buoy stations with the thermoresistor chains were installed several times at the depths 24–28 m in the corners of a triangle with the sides that varied from setting to setting in the range from 40 to 130 m. Frequent (every 10 s) temperature measurements were performed by highly sensitive sensors spaced vertically at a distance of about 1 m from each other. Data processing made it possible to identify more than 50 recorded cases of IW packages with the 1–10 m amplitude of oscillations, at that they were observed most often in spring (during the thermocline development). The values of the IW oscillation period, phase velocity of their propagation (magnitude and direction), length and amplitude, and also their number in a package were calculated.

Conclusions. It was revealed that the IW packages propagate mainly from the deep part of the sea to the coast. They are often observed in the frontal zones related to the intrusion of warmer or colder waters to the thermoresistor chains location area. The IW phase velocity was established to be in a statistically significant dependence on the temperature stratification parameters as well as on the IW nonlinearity parameter.

Keywords: Black Sea, shelf, thermoresistor chain cluster, long-term measurements, temperature stratification, internal wave package, thermoresistor chain, internal waves

Acknowledgements: The study was carried out within the framework of state assignment of IO RAS FMWE-2021-0013 and supported by the RSF grant No. 23-17-00056.

For citation: Ocherednik, V.V. and Zatsepin, A.G., 2023. Packages of Short-Period Internal Waves on the Black Sea Shelf Based on the Measurement Data of the Thermoresistor Chains Cluster. *Physical Oceanography*, 30(5), pp. 612-631.

© V. V. Ocherednik, A. G. Zatsepin, 2023

© Physical Oceanography, 2023

Introduction

Among short-period and submesoscale hydrophysical processes in natural stratified water bodies, internal waves (IWs) occupy a special place. Firstly, this is the most well-organized and regular process with a pronounced oscillatory character. Secondly, this is one of the fastest mechanisms for transferring energy and momentum in the water column over a long distance. Thirdly, and most



importantly, IW instability and collapse are one of the main energy sources for small-scale turbulent mixing of ocean waters [1].

Despite the fact that IWs have been the object of close research for many decades, their patterns, formation, and destruction mechanisms are not fully understood [2, 3]. This, in particular, applies to short-period IWs on the Black Sea shelf, although they have been studied by many specialists using various research methods [2–23]. Despite the fact that the Black Sea is practically tideless, it has a developed IW field. In this case, the IW amplitude values are approximately smaller than in the ocean or tidal seas. Nevertheless, intense IWs also occur here [4, 5].

Thermoresistor chains (TRCs) are often used to study hydrophysical processes, including IWs. Numerous publications describe the use of permanently installed TRCs placed on stationary platforms [13, 24], drifting buoys [22, 25, 26] or on vessels moving at low speed [27, 28]. Permanently installed TRCs are an effective tool for studying both seasonal and interannual temperature variability, as well as short-term ones on a scale from several seconds to several days. In Russia, shelf-based TRCs were successfully used in the study of short-period hydrophysical processes in the Black and Baltic Seas [20, 21, 29].

In the present paper, unlike many other studies, the measurement of the characteristics of short-period IWs was carried out using not a single shelf-based TRC, but a shelf-based thermoresistor cluster (hereinafter referred to as the “cluster”), long-term installed on the shelf of the northeastern Black Sea in the Golubaya Bay area [30].

Before the experiment, the data obtained, as well as the presentation of the measurement results and their analysis will be described, it should be noted that an experiment with high-frequency thermoresistor measurements of vertical temperature distributions, very similar in method and unique for that time, was carried out by Yu. A. Ivanov and B. N. Filyushkin with the participation of a number of employees of the Institute of Oceanology of the Academy of Sciences of the Soviet Union in the Black Sea in the Golubaya Bay area back in 1966–1967. In this experiment, a cluster of three TRCs was installed a little further from the coast (at a distance of 1500 m) than in this work with a distance of about 100 m between them. The TRCs were connected to an underwater cable that led to the shore, where the information from them was recorded by a self-recording unit. Each TRC consisted of six semiconductor sensors located at a distance of 5 m from each other. The measurement resolution was 2 minutes, the accuracy was 0.1°C. The installation of the thermoresistor cluster continued for 35 days in the summer. The fourth TRC was located on the Froude buoy, and the information from it was transmitted via cable to the vessel, which was drifting in the deep sea at various time periods during the operation of the thermoresistor cluster. Results of the measurement data processing and analysis using a TRC on a drifting Froude buoy are described in [14, 19], and using a shelf-based thermoresistor cluster – in [6]. Analysis of the results of statistical measurement data processing gave grounds to draw the following conclusions: temperature fluctuations in the considered

frequency range, specific for IWs, have a well-defined intermittency in time, that is, time intervals with a large amplitude of fluctuations are replaced by time intervals with a small amplitude; the energy of temperature fluctuations depends significantly on stratification and reaches a maximum for all frequencies considered in the layer of maximum vertical temperature gradient; at some time intervals, there is a fairly high coherence of temperature fluctuations measured by various sensors, both vertically and horizontally. Using phase relationships for series with high coherence, the IW parameters, in particular their length and phase velocity, were calculated.

The aim of the paper is to calculate and analyze the characteristics of short-period IW packages based on the data from long-term measurements of vertical temperature distributions by a cluster of three moored TRCs spaced apart on the Black Sea shelf in the Golubaya Bay area.

In the research results described in this paper, owing to high frequency of temperature measurements, high accuracy, and vertical resolution, it was possible to reliably identify several dozen cases of propagation of short-period IW packages (from three fluctuations in a package or more) and evaluate not statistically, but individually for those waves, which were observed on all three moored TRCs in the cluster, such parameters as amplitude, period, length, and phase velocity. In addition, a statistically significant dependence of the IW phase velocity on the temperature stratification parameters, as well as on the IW nonlinearity parameter, was established. It is shown that most often regular IW packages are observed near fronts formed by tongues of warmer or colder waters invading the area where the thermoresistor cluster is located.

Brief description of TRCs and their location in the cluster

Location scheme of TRCs in the cluster on the map is shown in Fig. 1, *a*.

The cluster was located in the water area of the Gelendzhik Polygon [1] at the bottom, at a depth of about 26 m, from 2018 to 2020. TRCs were installed at the vertices of a triangle with sides that were not equal to each other and varied from installation to installation, with a length from 40 to 130 m. TRCs were connected to a multi-modem station [31], which, in turn, was connected to an armoured fiber-optic cable with two conductive cores, through which electrical power was supplied to the devices and prompt measurement data transmission to the on-shore server.

Each TRC, 20 m long, consists of 21 temperature sensors and 3 pressure sensors (on the upper, middle, and lower horizons), coupled in a single housing with temperature sensors located on the same horizons. The sensors are placed at the same distance from each other, which is approximately 1 m. TRCs are fixed to moored buoy stations with a subsurface buoy submerged to a depth of 5–6 m. The accuracy of temperature measurements is about 0.01°C, the measurement period is 10 s. A detailed description of TRCs is presented in [32]. A more detailed description of the cluster can be found in [33].

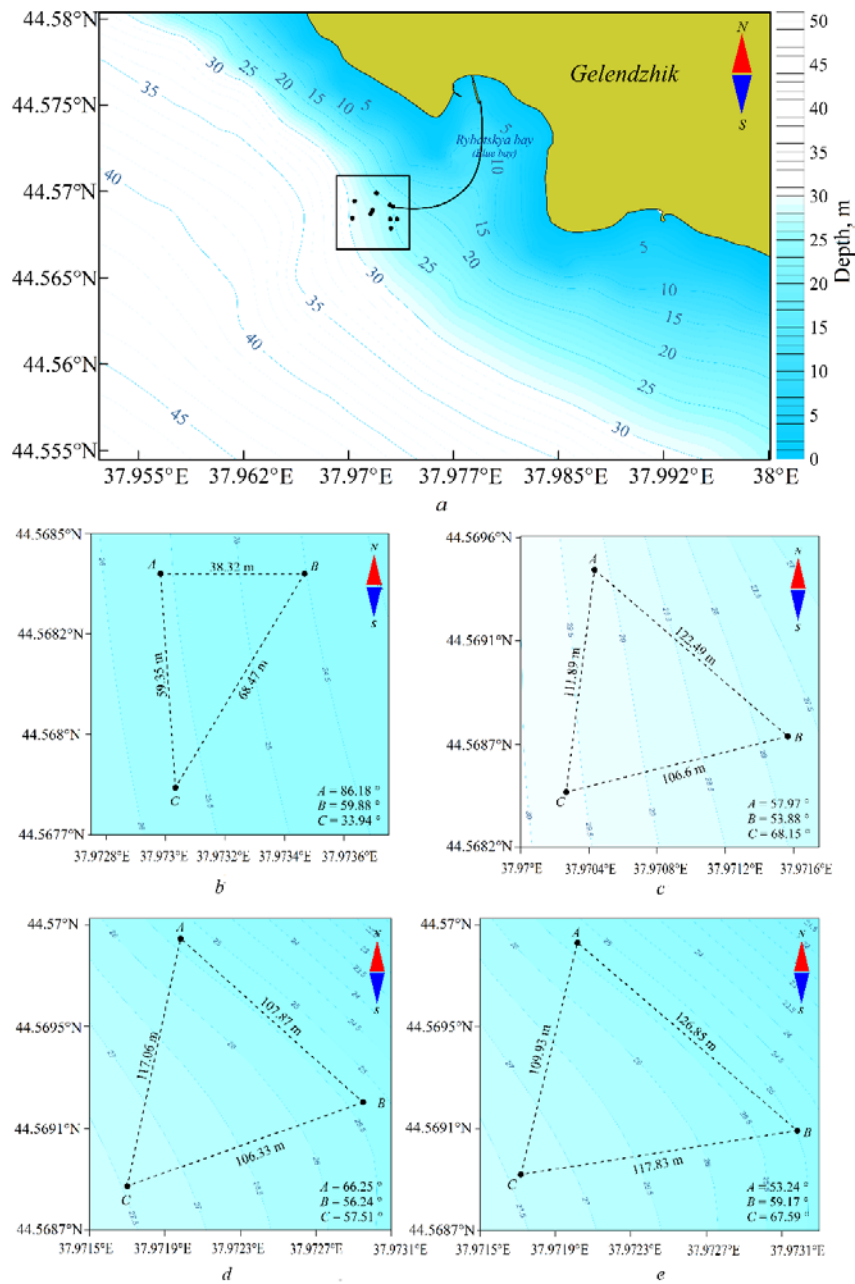


Fig. 1. Location (a) of the cluster of thermoresistor chains (points) and their configuration in the cluster from 24.04.2018 to 10.07.2018 (b), from 28.09.2018 to 17.02.2019(c), from 24.04.2019 to 15.05.2019 (d) and from 17.05.2019 to 02.06.2020 (e)

TRCs were installed from a motor boat board. In this case, the first thing the TRC was connected to was an outlet cable, the end of which was previously marked with a surface drifter. After this, the TRC was turned on from the shore module. After checking the connection and initializing the operation of the sensors, a moored buoy station, on which the TRC was located, was installed. In this case,

the subsurface buoy with a TRC was gradually etched overboard along its entire length. The buoy moved away from the boat with the current, and the boat running slowly moved to the intended point of the station setting. When the boat arrived at this point, the buoy station anchor was thrown overboard. Sinking to the bottom, the anchor pulled the TRC and the buoy along with it. When the anchor reached the bottom, the buoy rope was tightened and the TRC acquired a position close to vertical. The buoy was located at a depth of 5–6 m from the sea surface. After this, the coordinates of the station location were specified. The same operation was carried out when installing two other TRCs.

According to Fig. 1, the first cluster configuration is far from a regular triangle and is very different from its configuration in subsequent formulations. This is due to the fact that the transmitting and receiving cables from the multi-modem station to TRCs *A* and *B* were not long enough, and for TRC *C* the cable was already extended, which made it possible to take it and the TRC connected to it to a greater distance from the multi-modem station. It should also be noted that the wind drift of the boat makes it difficult to install the station at the chosen point, so the actual configuration of the TRCs in the cluster is always somewhat different from the intended one.

Measurement data and their use for calculation of IW parameters

The work analyzed the data of TRCs obtained from April 2018 to June 2020 (Fig. 2). IW packages were recorded mainly in spring months during the seasonal thermocline formation. In autumn, it was not possible to detect IWs due to the temperature jump layer deepening to a depth over 20 m. At the same time, significant temperature changes were observed only in the bottom layer, being displayed on 1–2 temperature sensors located directly above the bottom.

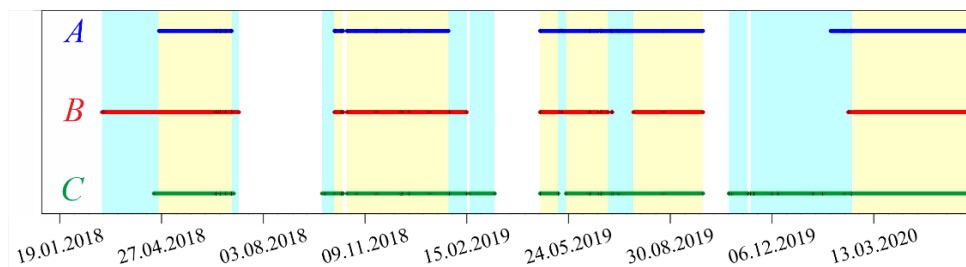


Fig. 2. Periods of measurement by thermoresistor chains in the cluster: three thermoresistor chains (yellow color), one or two thermoresistor chains (blue color). *A*, *B* and *C* are thermoresistor chains (see Fig. 1, *a*)

Examples of recorded IWs, as well as corresponding temperature profiles at the beginning and at the end of the measurement cycle are shown in Figs. 3–6. The recorded IW packages were divided according to the types of their manifestation:

- in the upper layer (Fig. 3);
- in the bottom layer (Fig. 4);
- in the thermocline column (Fig. 5);
- in the entire water column (Fig. 6).

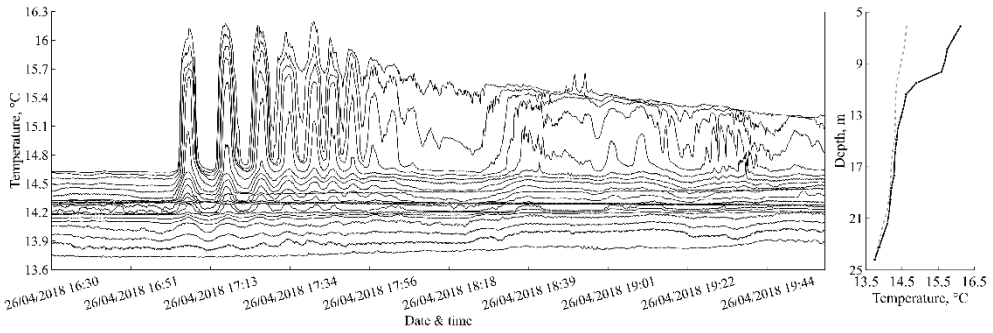


Fig. 3. An example of the high-amplitude IW package in the upper layer: *on the left* – time unrolling of temperature sensor readings at one of the thermoresistor chains on April 26, 2018 from 16:30 to 20:00; *on the right* – vertical temperature distributions at the beginning (dashed line) and at the end (solid line) of the presented measurement period

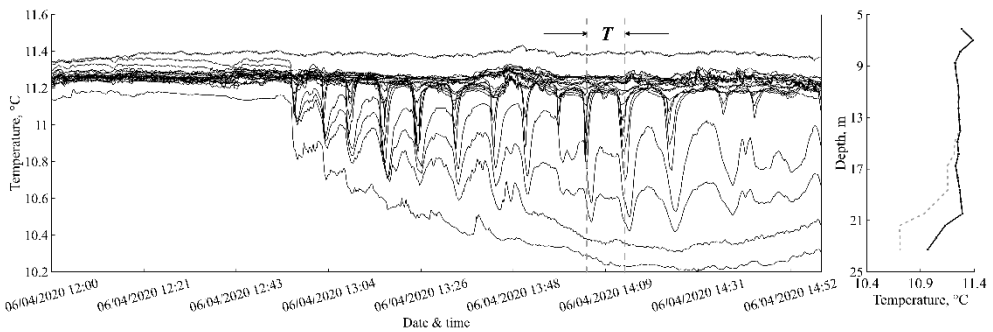


Fig. 4. An example of the high-amplitude IW package in the lower layer: *on the left* – time unrolling of temperature sensor readings at one of the thermoresistor chains on April 6, 2020 from 12:00 to 15:00 (letter *T* denotes the IW period – the time between two temperature minima at one and the same sensor); *on the right* – vertical temperature distributions at the beginning (dashed line) and at the end (solid line) of the presented measurement period

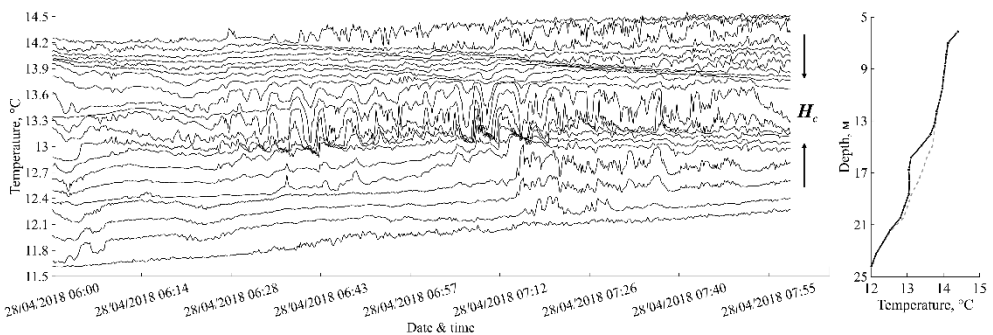


Fig. 5. An example of the low-amplitude IW package concentrated mainly within the intermediate layer of H_c thickness in the thermocline: *on the left* – time unrolling of temperature sensor readings at one of the thermoresistor chains on April 28, 2018 from 06:00 to 08:00; *on the right* – vertical temperature distributions at the beginning (dashed line) and at the end (solid line) of the presented measurement period

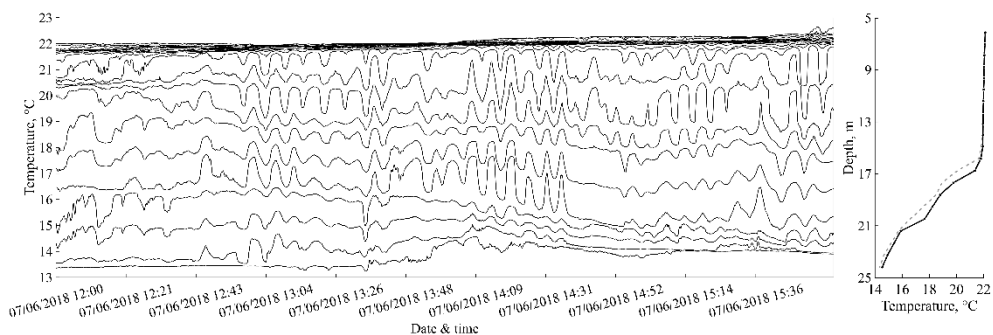


Fig. 6. An example of the low-amplitude IW packages covering almost the entire thermocline: *on the left* – time unrolling of temperature sensor readings at one of the thermoresistor chains on June 7, 2018 from 12:00 to 16:00; *on the right* – vertical temperature distributions at the beginning (dashed line) and at the end (solid line) of the presented measurement period

Calculation of IW parameters in packages

When processing IW measurement data, the values of their period T_{iw} , amplitude a , and phase velocity of propagation c were calculated.

The IW period was calculated as the time interval between adjacent temperature maxima or minima at the same sensor. Fig. 7 shows a histogram of calculated periods, distributed into groups with a step of 2 minutes.

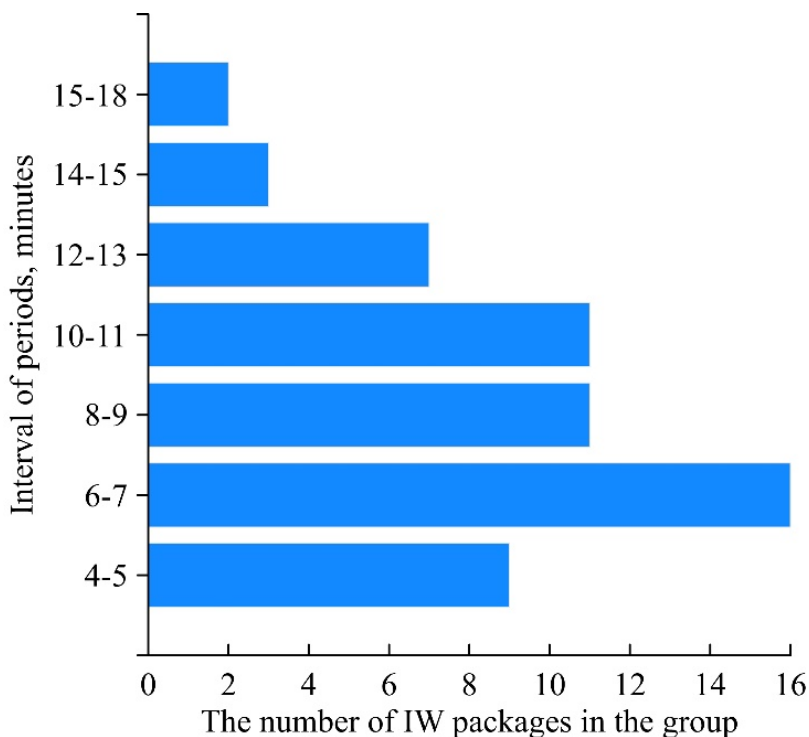


Fig. 7. Relationship between the IW periods and the number of packages

The IW periods are divided into groups of 2 minutes. It is necessary to find out which periods are recorded most often. In this case, the minimum period is 4.25 minutes (255 s), and the maximum is 17.15 minutes (1029 s). According to Fig. 7, most of the recorded packages have a period from 5 to 12 minutes and in rare cases about 15 or more.

The IW amplitude, that is, their range, was calculated based on the manifestation of temperature fluctuations at the sensors at a distance between adjacent sensors of 0.95–1.05 m. This took into account the reduction in the vertical distance between the sensors (up to 0.85 m) due to the tilt of the TRC caused by intense current.

Two methods were used to estimate the IW amplitude. In the first method, it was assumed that in the absence of IWs, temperature value T_m ($1 \leq m \leq 21$) at any of the sensors is quasi-constant (changes little over time). During the passage of an IW package, it periodically changes from T_{m0} ($t = 0$), undisturbed value, to $T_{m\tau}$ ($t = \tau$), maximum changed value, where t is current moment in time, and τ is half of the fluctuation period. Difference $\Delta T_m = T_{m0} - T_{m\tau}$ was estimated, and temperature difference $\Delta T_{mk} = T_m(0) - T_k(0)$ between the sensors at horizons m and k in undisturbed conditions was selected such that $\Delta T_{mk} \approx \Delta T_{m\tau}$. It was assumed that the IW amplitude at the horizon was $m a = (m - k)\Delta z$ in absolute value. Obviously, minimum value a determined by this method is Δz , i.e., it allows determining the IW amplitude exceeding 0.85–1.05 m. This value is an error in determining the amplitude at horizon m .

Another method for the IW amplitude estimate, more familiar to oceanologists, used the change in the position of a selected isotherm over time. Its vertical displacement was estimated from the initial position at $t = 0$ to the maximum deviation at $t = \tau$. As when constructing isotherms based on the readings of temperature sensors at fixed horizons, the error in determining the position of the isotherms can also reach value Δz in the range of 0.85–1.0 m, the error when using both the first and second methods is approximately the same.

Both estimation methods produced well comparable results. Ultimately, the first of the methods discussed above was used to estimate the IW amplitude (span).

IW phase velocity c (module and direction) was calculated using the algorithm described in [33]. This algorithm uses the delay time for the passage of a certain IW phase through two other TRCs relative to the initial phase.

Wavelength λ was calculated based on its definition, from which it follows that $\lambda = c \cdot T_{iw}$.

Mean values of parameters λ , c , T_{iw} , and a for each observed IW package are given in Table. The values of Brunt-Väisälä frequency N_T averaged over the water layer depth are also given there, calculated from the temperature profile using the following formula:

$$N_T = \sqrt{g\alpha \frac{\Delta T}{H_o}}$$

where α is coefficient of thermal expansion (CTE) of sea water; T is temperature; ΔT is temperature difference between upper and lower sensors; H_o is polygon depth, which is considered constant at the polygon scale and equal to 26 m. Table also shows the values of another parameter H_c , the thickness of the layer which intra-wave fluctuations were observed in (see Fig. 5).

IW characteristics resulted from the studies

Date	T_{iw} , s	c , m/s	λ , m	$\alpha \cdot 10^4$	H_c , m	N_T , 1/s	ΔT , °C	α , m
26.04.2018	600	0.06	39	1.96	10.5	0.0132	2.38	6.5
28.04.2018	320	0.13	41	1.75	15.0	0.0116	2.03	4.3
29.04.2018	700	0.12	86	1.88	9.0	0.0151	3.22	4.9
30.04.2018	514	0.06	29	1.85	18.5	0.0113	1.83	7.6
01.05.2018	440	0.17	76	1.89	16.0	0.0111	1.75	2.7
02.05.2018	600	0.17	104	1.89	17.5	0.0159	3.56	4.3
03.05.2018	432	0.14	62	1.95	13.0	0.0167	3.81	3.3
04.05.2018	554	0.05	25	1.97	10.5	0.0181	4.42	4.3
04.05.2018	451	0.11	49	1.94	8.0	0.0175	4.16	2.2
05.05.2018	600	0.09	51	1.92	16.0	0.0163	3.64	5.4
12.05.2018	300	0.09	28	1.84	20.5	0.0136	2.66	7.6
14.05.2018	480	0.07	34	2.05	23.5	0.0129	2.16	3.3
19.05.2018	352	0.09	30	2.17	15.0	0.0229	6.43	4.9
20.05.2018	400	0.36	144	2.12	12.5	0.0225	6.32	3,3
28.05.2018	467	0,08	39	2.12	15.0	0.0147	2.71	4.3
28.05.2018	467	0.19	89	2.06	20.5	0.0165	3.49	2.2
28.05.2018	400	0.27	110	2.05	15.0	0.0186	4.48	2.2
29.05.2018	338	0.11	36	1.96	23.5	0.0166	3.73	8.7
31.05.2018	600	0.10	58	2.03	10.5	0.0088	1.02	8.7
01.06.2018	520	0.14	73	1.9	8.0	0.0103	1.49	2.2
01.06.2018	533	0.10	51	1.86	9.0	0.0111	1.76	7.6
02.06.2018	450	0.27	120	1.92	15.0	0.0143	2.85	4.3
07.06.2018	255	0.27	58	2.49	15.0	0.0271	7.86	2.2
07.06.2018	379	0.15	57	2.51	17.0	0.0268	7.58	3.3
29.04.2019	808	0.13	101	1.66	21.0	0.0114	2.09	5.4
30.04.2019	417	0.13	53	1.71	21.0	0.0139	2.97	2.2
30.04.2019	480	0.12	55	1.69	21.0	0.0151	3.57	2.7
26.05.2019	427	0.37	157	2.27	18.0	0.0256	7.67	6.5
15.06.2019	600	0.39	235	2.79	12.5	0.0397	14.98	8.7

The primary values of sea water CTE α depending on its temperature were taken from Table 4.1 of the work¹. More accurate values were obtained by interpolating data for water salinity characteristic of the Black Sea shelf zone in the Gelendzhik region.

In total, during the research period, 56 IW packages were identified. Table presents those of them that were used to analyze their phase velocity (29 packages). IW packages recorded on only one or two TRCs, as well as those packages that consisted of less than three waves, were filtered out.

A comparison of the period of intrawave fluctuations T_{iw} with the period of free fluctuations of particles in the Brunt-Väisälä stratified aquatic environment $T_{VB} = 2\pi/N_T$ showed that in the vast majority of cases $T_{iw} > T_{VB}$, as it should be for internal waves. However, there are some exceptions; they may be associated with failure to take into account salinity stratification, which in spring can account for one third of thermal stratification [34], as well as with the influence of current velocity.

The magnitude of the IW phase velocity and its direction are shown in Fig. 8.

The figure shows that the vast majority of IW packages propagate towards the shore. Nevertheless, it is clear that some wave packages propagated predominantly along the coast.

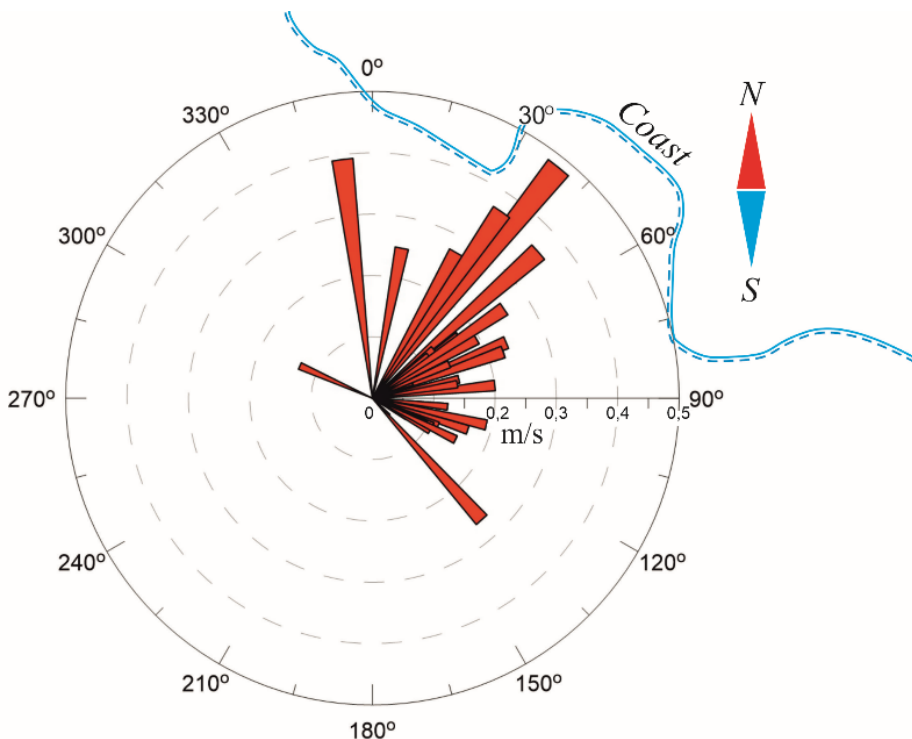


Fig. 8. IW propagation direction and velocity module

¹Kondratyeva, V.I., 1975. [Oceanographic Tables]. 4th Edition, Revised. Leningrad: Gidrometeoizdat, 477 p. (in Russian).

IW phase velocity parametrization

In a deep two-layer temperature-stratified sea, where $H_c/H_o \ll 1$ and $\lambda/H_o \ll 1$, from considerations of dimensionality and self-similarity, the IW phase velocity should be determined by the following expression:

$$c = A\sqrt{g'H_c}.$$

Here, A is numeric constant; $g' = g\alpha\Delta T$, where ΔT is temperature jump at the layer boundary; H_c is “warm” layer thickness at the boundary of which IWs are observed; H_o is sea depth.

However, on a relatively shallow shelf, the above inequalities do not hold. It will be assumed that in the present case the dependence of the phase velocity of IW on external parameters is determined by the following expression:

$$c = AN_T H_o \left(\frac{H_c}{H_o}\right)^m. \quad (1)$$

Expression (1) uses the assumption that the phase velocity is proportional to the product of the mean buoyancy frequency over water layer thickness N_T , water layer thickness H_o , and power-law dimensionless parameter H_c/H_o , where H_c is thickness of the layer in which IWs are observed, and H_o is location depth. In this case, A, m are numerical constants, the values of which should be determined by analyzing measurement data.

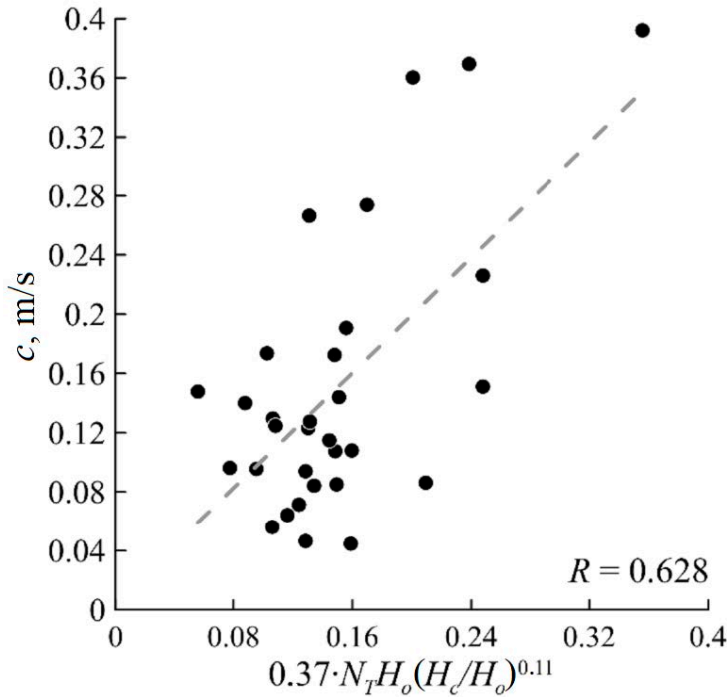


Fig. 9. Regression dependence of c on value $0.37N_T H_o \left(\frac{H_c}{H_o}\right)^{0.11}$ with correlation coefficient $R = 0.628$

To determine constant m , dependence $c = AN_T H_o \left(\frac{H_c}{H_o}\right)^m$ should be analyzed. As a result, it can be concluded that the best correlation between right and left parts of this dependence is achieved at $A = 0.37$ and $m = 0.11$ (Fig. 9).

Since dependence c from parameter H_c/H_o is very weak, it can be neglected and considered that $c = AN_T H_o$ (Fig. 10).

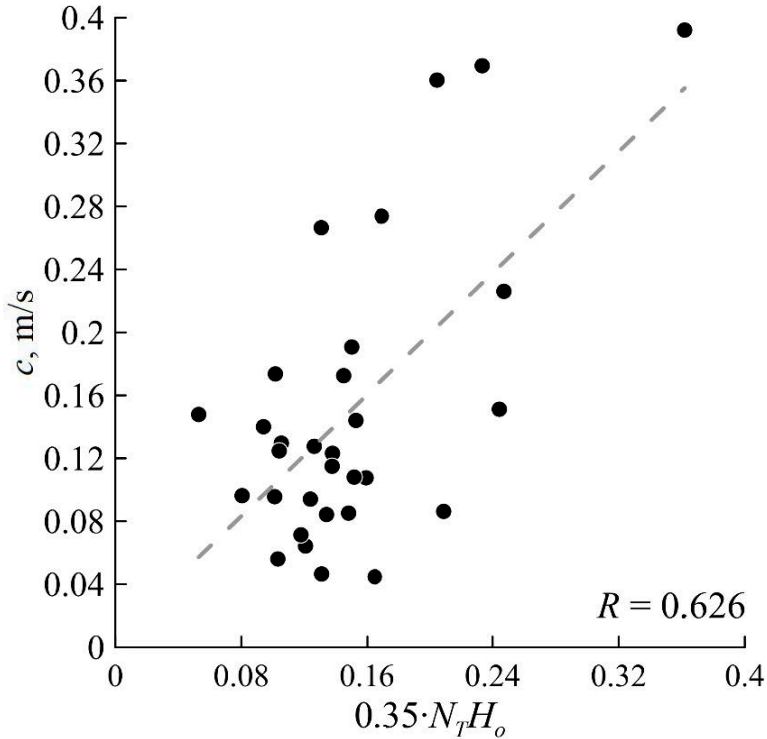


Fig. 10. Correlation dependence of c on $AN_T H_o$ at $A = 0.35$ ($R = 0.626$ is correlation coefficient)

It is obvious that, statistically this dependence is provided no worse than a more complex one, taking into account the thickness of the IW propagation layer. In addition, the obtained dependence corresponds well to the theoretical one:

$$c = \frac{N_T H_o}{\pi}.$$

It follows that on the inner shelf the speed of IW propagation is mainly determined by the depth-average stratification of the water layer and its thickness. This makes it possible to estimate the phase velocity of IWs based on the location depth and mean temperature gradient without using additional data.

Since the selected IW packages generally had a significant fluctuation amplitude, it makes sense to check the dependence of the phase velocity of wave propagation on their amplitude, that is, on parameters a/H_o and a/λ . In this case, the first parameter to some extent characterizes the influence of the dynamic resistance of a relatively shallow-water environment to propagating high-amplitude

waves, and the second – the influence of the wave nonlinearity on its propagation speed.

The dependences of value $c/(N_T H_o)$ on a/H_o and a/λ in logarithmic coordinates are presented in Fig. 11.

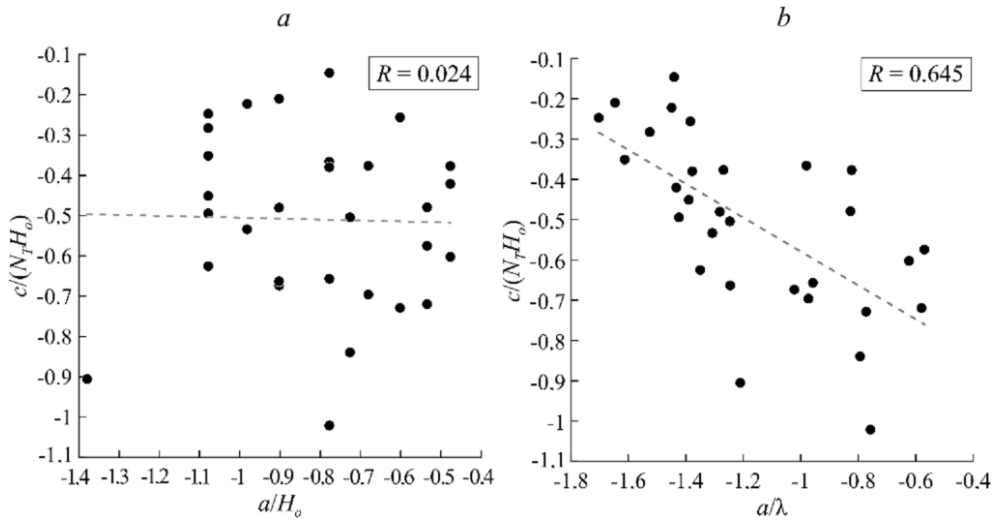


Fig. 11. Dependence of value $c/(N_T H_o)$ on a/H_o (a) and on a/λ (b). Dashed line is regression line

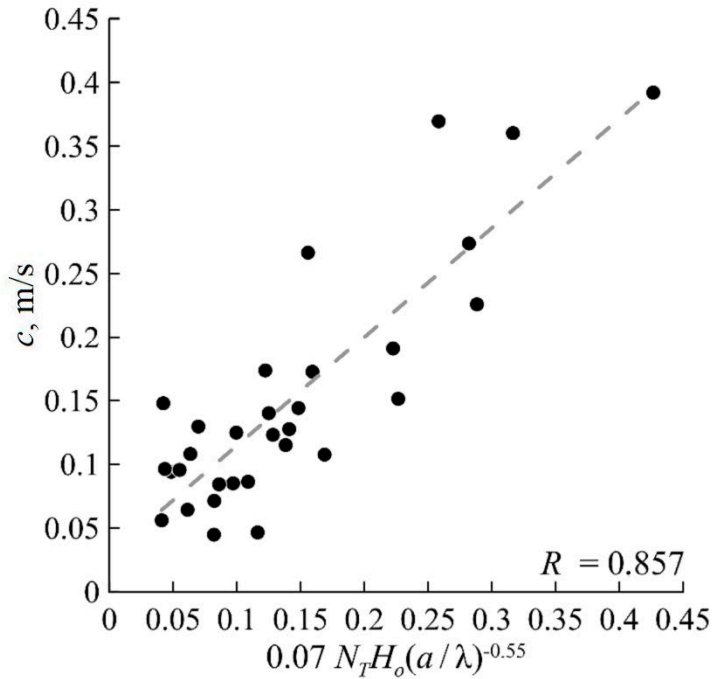


Fig. 12. Refined dependence of phase velocity on parameters $N_T H_o$ and a/λ

According to Fig. 11, *a*, it is clear that there is practically no dependence of the dimensionless phase velocity of waves on parameter a/H_o and it can be neglected. However, the nonlinearity wave parameter (Fig. 11, *b*) significantly affects its propagation speed, and more nonlinear waves propagate more slowly than less nonlinear ones. The physical meaning of this dependence is not clear to the authors and requires further study.

As a result, the refined dependence of the phase velocity of IW propagation on parameters $N_T H_o$ and a/λ can be represented as follows:

$$c = 0.07 N_T H_o \left(\frac{a}{\lambda} \right)^{-\frac{1}{2}}.$$

The graph of this dependence is shown in Fig. 12. It shows how much the correlation between the measured phase velocity of the IW and its parameterization improved.

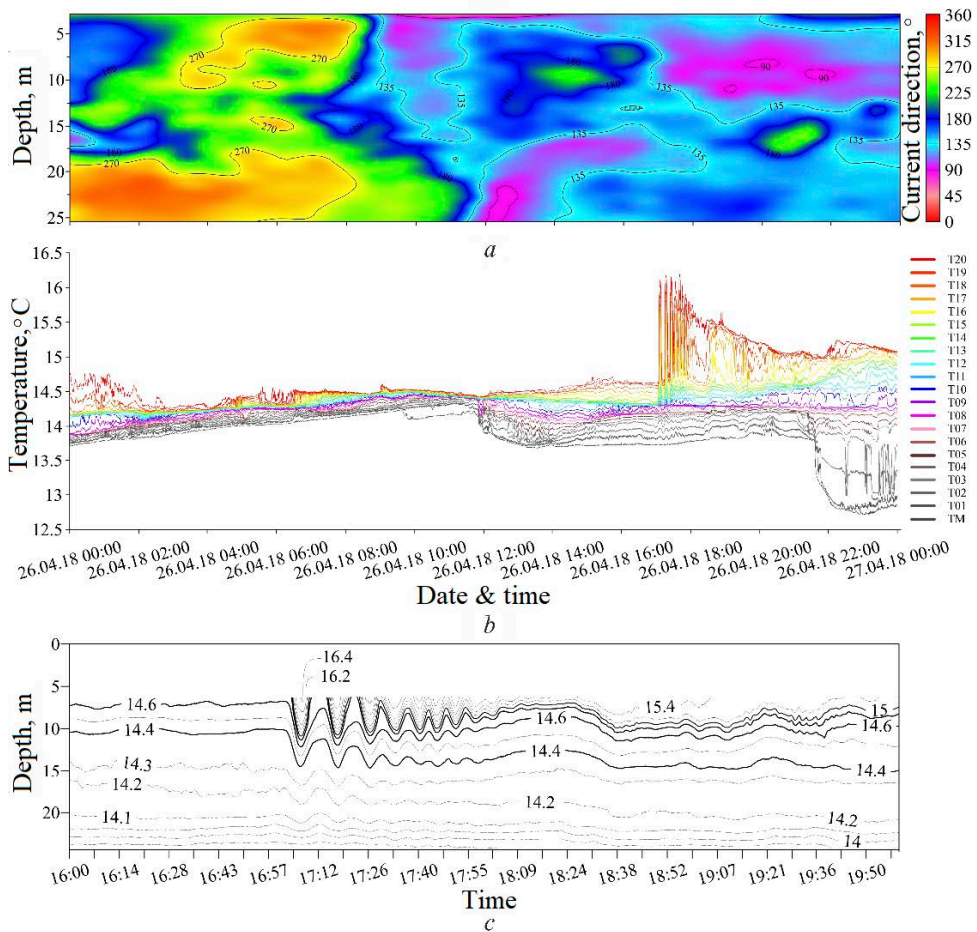


Fig. 13. Representation of the time-coupled ADCP measurement data (vertical and temporal distribution of current direction) (*a*); readings of thermoresistor chain *B* thermal sensors on April 26, 2018 (from top to bottom: T20 – TM are thermal sensors where T20 is the top sensor and TM is the bottom one) (*b*); isotherm fluctuations in the IW package in the upper layer from 17:00 to 18:00 (*c*)

As already noted, subsequently it is desirable to take into account not only the temperature, but also the salinity contribution to density in estimating the Brunt-Väisälä frequency and calculate the IW propagation speed based on its estimation along the “full” density gradient. In addition, it seems important to take into account the influence of current velocity on the IW propagation speed. Since the propagation of IWs was directed mainly perpendicular to the coast, and the current velocity component in this direction is small [35], then, apparently, the current velocity influence in most cases was insignificant. Nevertheless, we will try to take it into account in further research.

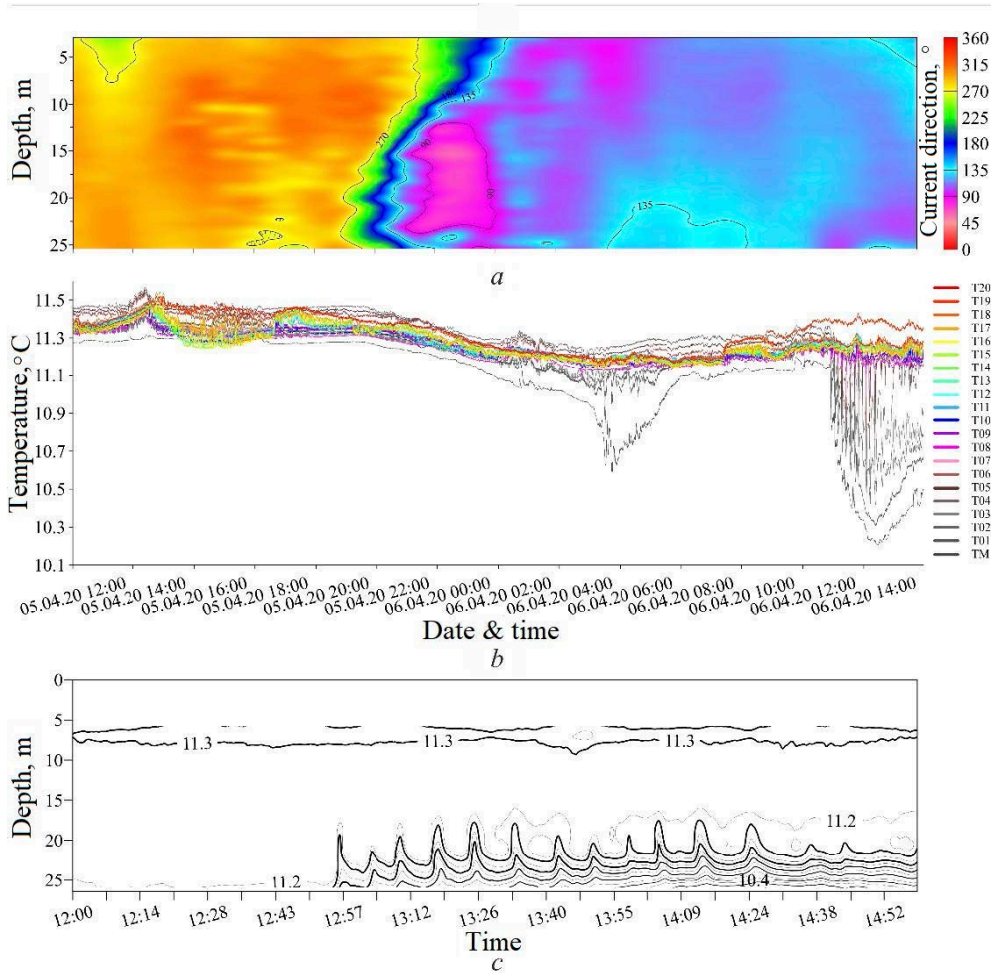


Fig. 14. Representation of the time-coupled ADCP measurement data (vertical and temporal distribution of the current velocity direction) (a); readings of thermoresistor chain B thermal sensors on April 06, 2020 (see designations in Fig. 13) (b); isotherm fluctuations in the IW package in the lower layer from 13:00 to 15:00 (c)

In conclusion, it is noted that, although the formation mechanisms of the observed IW packages were most likely different, their appearance in the cluster area in many cases was preceded by a change in the current velocity

sign (Figs. 13, 14). Current velocity was measured in the cluster area using a bottom acoustic Doppler current profiler (ADCP), also connected to a multi-modem station. As is known, a change in the current velocity sign in the coastal zone of the northeastern Black Sea most often occurs due to the Black Sea Rim Current meandering and the formation of mesoscale anticyclonic eddies [35]. Figs. 13 and 14 show cases when the northwestern direction of the current changed to the southeastern one before the appearance of IW packages. This means that IW packages were apparently observed in the frontal zones of anticyclonic eddies. This assumption is consistent with what was previously stated that many IW packages are observed in the area of warmer or colder water tongues invading the cluster water area. It is possible that these tongues and the eddies that generate them are the energy source of IWs, as previously indicated in [15], but this issue requires special research.

Main results and conclusions

1. Analysis of the spatiotemporal variability of temperature stratification of waters on the inner Black Sea shelf was carried out based on measurement data from a TRC cluster manufactured at the Southern Branch of the Institute of Oceanology of the Russian Academy of Sciences. The measurements were carried out in 2018–2020. The cluster consisted of three TRCs at moored buoy stations, installed at depths of 24–28 m at the vertices of a triangle with its sides 40–130 m long. TRCs, about 20 m long, made frequent (once every 10 seconds) temperature measurements using sensitive sensors located along verticals with a distance of less than 1 m.

2. It was established that the IW packages were one of the factors causing strong short-period variability in temperature stratification in spring and early summer (April – June). Measurement data processing permitted to identify 56 IW packages over the entire measurement period. During the indicated season of the year, IW packages were observed 7–10 times a month. In summer and autumn seasons, the occurrence of IWs on the inner shelf was significantly less common, possibly due to the upper quasi-homogeneous layer deepening and lowering of the thermocline to the bottom.

3. The IW period, length, and amplitude values, the value and direction of their phase propagation velocity were calculated, and the number of IWs in the package was estimated. It turned out that IWs predominantly spread from the deep-sea part to the coast and were often found in frontal zones associated with the invasion of warmer or colder waters into the cluster water area. The values of the IW phase velocity modulus varied in the range from 5 to 40 cm/s. In this case, the wavelength varied from 25 to 250 m, the amplitude – from 1 to 10 m. The number of waves in the package varied from 3 to 16. Single wave disturbances were not taken into account.

4. Statistically assured dependence of the phase velocity of IWs on the temperature stratification parameters, sea depth in the region of the cluster location, as well as on the wave nonlinearity parameter was established. It has

the following form: $c = 0.07 N_T H_o \left(a/\lambda \right)^{-\frac{1}{2}}$. From this dependence, it follows that with an increase in the nonlinearity parameter, the phase velocity of IW propagation decreases. This fact requires a physical explanation.

5. Although the formation mechanisms of the observed IW packages were most likely different, their appearance in the cluster area was often preceded by a change in the current velocity sign. In a number of cases, IW packages were observed in the frontal zones of anticyclonic eddies. Perhaps, these are the energy source for the IW formation. However, this issue requires further research.

6. In the future, it seems important to take into account not only the temperature, but also the salinity contribution to density in the water layer stratification estimate and to calculate the IW propagation speed based on the Brunt-Väisälä frequency estimate along the density gradient. In addition, it seems important to take into account the influence of current velocity on the IW propagation speed.

7. It is advisable to install an additional TRC cluster outside the shelf zone in deep water so that the bottom does not limit thermocline position and its inherent intra-wave fluctuations, and to study the statistics and physical patterns of the appearance of IW packages throughout the warm period of the year.

REFERENCES

1. Zatsepin, A.G., Ostrovskii, A.G., Kremenetskiy, V.V., Nizov, S.S., Piotukh, V.B., Soloviev, V.A., Shvov, D.A., Tsibul'skiy, A.L., Kuklev, S.B. [et al.], 2014. Subsatellite Polygon for Studying Hydrophysical Processes in the Black Sea Shelf-Slope Zone. *Izvestiya, Atmospheric and Oceanic Physics*, 50(1), pp. 13-25. <https://doi.org/10.1134/S0001433813060157>
2. Konyaev, K.V. and Sabinin, K.D., 1992. [*Waves inside the Ocean*]. St.-Petersburg: Gidrometeoizdat, 272 p. (in Russian).
3. Sabinin, K.D., Serebryanyi, A.N. and Nazarov, A.A., 2004. Intensive Internal Waves in the World Ocean. *Oceanology*, 44(6), pp. 753-758.
4. Bondur, V.G., Serebryany, A.N. and Zamshin, V.V., 2018. An Anomalous Record-High Internal Wave Train on the Black Sea Shelf, Generated by an Atmospheric Front. *Doklady Earth Sciences*, 483(2), pp. 1519-1523. doi:10.1134/S1028334X18120012
5. Bondur, V.G., Serebryany, A.N., Zamshin, V.V., Tarasov, L.L. and Khimchenko, E.E., 2019. Intensive Internal Waves with Anomalous Heights in the Black Sea Shelf Area. *Izvestiya, Atmospheric and Oceanic Physics*, 55(1), pp. 99-109. doi:10.1134/S000143381901002X
6. Byshev, V.I., Ivanov, Yu.A. and Morozov, Ye.G., 1971. Study of Temperature Fluctuations in the Frequency Range of Internal Gravity Waves. *Izvestiya, Atmospheric and Oceanic Physics*, 7(1), pp. 25-30.
7. Ivanov, V.A. and Lisichenok, A.D., 2002. Internal Waves in the Shelf Zone and near the Shelf Edge in the Black Sea. *Physical Oceanography*, 12(6), pp. 353-360. doi:10.1023/A:1021733330076
8. Ivanov, V.A. and Lisichenok, A.D., 2000. [On the Mechanism of Generation of Short-Period Internal Waves by Wind Pulsations]. In: MHI, 2000. *Ekologicheskaya Bezopasnost' Pribrezhnoy i Shel'fovoy Zon i Kompleksnoe Ispol'zovanie Resursov Shel'fa* [Ecological Safety of Coastal and Shelf Zones and Comprehensive Use of Shelf Resources]. Sevastopol: MHI. Vol. 1, pp. 191-196 (in Russian).

9. Ivanov, V.A. and Serebryanyy, A.N., 1982. Frequency Spectra of Short-Period Internal Waves in a Nontidal Sea. *Izvestiya, Atmospheric and Oceanic Physics*, 18(6), pp. 527-529.
10. Ivanov, V.A. and Serebryanyi, A.N., 1983. Internal Waves on the Shallow Shelf in the Tideless Sea. *Izvestiya of the Academy of Sciences of the USSR. Atmospheric and Oceanic Physics*, 19(6), pp. 661-665 (in Russian).
11. Ivanov, V.A. and Serebryanyy, A.N., 1985. Short-Period Internal Waves in the Coastal Zone of a Nontidal Sea. *Izvestiya, Atmospheric and Oceanic Physics*, 21(6), pp. 496-501.
12. Ivanov, V.A. and Serebryany, A.N., 1985. Display of Small Amplitude Internal Waves on the Sea Surface. *Izvestiya of the Academy of Sciences of the USSR. Atmospheric and Oceanic Physics*, 21(7), pp. 795-799 (in Russian).
13. Serebryany, A.N. and Ivanov, V.A., 2010. Subsurface Waves Investigations from the Oceanographic Platform of the Marine Hydrophysical Institute of NAS of Ukraine during Thirty Years. In: MHI, 2010. *Ekologicheskaya Bezopasnost' Pribrezhnoy i Shel'fovoy Zon i Kompleksnoe Ispol'zovanie Resursov Shel'fa* [Ecological Safety of Coastal and Shelf Zones and Comprehensive Use of Shelf Resources]. Sevastopol: MHI. Vol. 21, pp. 146-156 (in Russian).
14. Ivanov, Yu.A., Smirnov, B.A., Tareev, B.A. and Filushkin, B.N., 1969. The Experimental Investigation of Temperature Oscillations in the Frequency Interval of Internal Gravity Waves. *Izvestiya of the Academy of Sciences of the USSR. Atmospheric and Oceanic Physics*, 5(4), pp. 416-425 (in Russian).
15. Lavrova, O.Yu., Mityagina, M.I. and Sabinin, K.D., 2008. [Possible Mechanisms of Internal Wave Generation in the Northeastern Part of the Black Sea]. *Current Problems in Remote Sensing of the Earth from Space*, 5(2), pp. 128-136 (in Russian).
16. Lavrova, O.Yu., Mityagina, M.I. and Sabinin, K.D., 2009. Manifestations of Internal Waves on the Sea Surface in North-Eastern Part of the Black Sea. *Issledovanie Zemli iz Kosmosa*, (6), pp. 49-55 (in Russian).
17. Lavrova, O.Yu., Mityagina, M.I. and Sabinin, K.D., 2011. Study of Internal Wave Generation and Propagation Features in Non-Tidal Seas Based on Satellite Synthetic Aperture Radar Data. *Doklady Earth Sciences*, 436(1), pp. 165-169. doi:10.1134/S1028334X11010272
18. Lavrova, O.Yu., Serebryany, A.N., Mityagina, M.I. and Bocharova, T.Yu., 2013. Subsatellite Observations of Small-Scale Hydrodynamic Processes in the Northeastern Black Sea. *Current Problems in Remote Sensing of the Earth from Space*, 10(4), pp. 308-322 (in Russian).
19. Navrotsky, V.V. and Filyushkin, B.N., 1969. Statistical Analysis of Temperature Time Fluctuations in the Sea Surface Layer. *Izvestiya of the Academy of Sciences of the USSR. Atmospheric and Oceanic Physics*, 5(7), pp. 714-723 (in Russian).
20. Serebryany, A.N. and Khymchenko, I.E., 2014. Observations of Internal Waves at Caucasus and Crimean Shelves of the Black Sea in Summer 2013. *Current Problems in Remote Sensing of the Earth from Space*, 11(3), pp. 88-104 (in Russian).
21. Silvestrova, K.P., Zatsepin, A.G. and Myslenkov, S.A., 2017. Coastal Upwelling in the Gelendzhik Area of the Black Sea: Effect of Wind and Dynamics. *Oceanology*, 57(4), pp. 469-477. doi:10.1134/S0001437017040178
22. Tolstosheev, A.P., Lunev, E.G. and Motyzhev, V.S., 2008. Development of Means and Methods of Drifter Technology Applied to the Problem of the Black Sea Research. *Oceanology*, 48(1), pp. 138-146. doi:10.1007/s11491-008-1016-4
23. Khimchenko, E.E. and Serebryany, A.N., 2018. Internal Waves on the Caucasian and Crimean Shelves of the Black Sea (According to Summer-Autumn Observations 2011-2016). *Journal of Oceanological Research*, 46(2), pp. 69-87. doi:10.29006/1564-2291.JOR-2018.46(2).7 (in Russian).
24. Myslenkov, S., Silvestrova, K., Krechik, V. and Kapustina, M., 2023. Verification of the Ekman Upwelling Criterion with In Situ Temperature Measurements in the Southeastern Baltic Sea. *Journal of Marine Science and Engineering*, 11(1), 179. doi:10.3390/jmse11010179

25. Motyzhev, S.V., Lunev, E.G. and Tolstosheev, A.P., 2011. The Development of Drift Technologies and Their Application to the Oceanographic Observations in the Black Sea and the World Ocean. In: MHI, 2011. *Ekologicheskaya Bezopasnost' Pribrezhnoy i Shel'fovoy Zon i Kompleksnoe Ispol'zovanie Resursov Shel'fa* [Ecological Safety of Coastal and Shelf Zones and Comprehensive Use of Shelf Resources]. Sevastopol: MHI of NAS of Ukraine. Iss. 24, pp. 259-272 (in Russian).
26. Serebryany, A.N. and Ivanov, V.A., 2013. Study of Internal Waves in the Black Sea from Oceanography Platform of Marine Hydrophysical Institute. *Fundamentalnaya i Prikladnaya Gidrofizika*, 6(3), pp. 34-45 (in Russian).
27. Centurioni, L.R., 2010. Observations of Large-Amplitude Nonlinear Internal Waves from a Drifting Array: Instruments and Methods. *Journal of Atmospheric and Oceanic Technology*, 27(10), pp. 1711-1731. doi:10.1175/2010jtecho774.1
28. Centurioni, L.R., 2018. Drifter Technology and Impacts for Sea Surface Temperature, Sea-Level Pressure, and Ocean Circulation Studies. In: R. Venkatesan, A. Tandon, E. D'Asaro, M. Atmanand, eds., 2018. *Observing the Oceans in Real Time*. Cham: Springer, pp. 37-57. doi:10.1007/978-3-319-66493-4_3
29. Munk, W. and Wunsch, C., 1998. Abyssal Recipes II: Energetics of Tidal and Wind Mixing. *Deep Sea Research Part I: Oceanographic Research Papers*, 45(12), pp. 1977-2010. doi:10.1016/S0967-0637(98)00070-3
30. Ocherednik, V.V., Silvestrova, K.P., Myslenkov, S.A. and Mashura, V.V., 2018. [Study of Internal Waves Using Data of Three Anchored Thermistor Chains]. In: V. A. Gritsenko, ed., 2018. *Coastal Zone of Sea: Studies, Management, Prospects. Proceedings of the International Youth Summer School*. Kaliningrad, pp. 12-16 (in Russian).
31. Baranov, V.I., Zatsepin, A.G., Kuklev, S.B., Ocherednik, V.V. and Zinchenko, A.V., 2017. Multiple System for On-Line Monitoring of Underwater Conditions. In: SIO RAS, 2017. *Proceedings of the XV All-Russian Scientific and Technical Conference "MSOI-2017": Modern Methods and Means of Oceanological Research*. Moscow: SIO RAS. Vol. 2, pp. 287-289 (in Russian).
32. Ocherednik, V.V., Baranov, V.I., Zatsepin, A.G. and Kuklev, S.B., 2018. Thermochains of the Southern Branch, Shirshov Institute of Oceanology, Russian Academy of Sciences: Design, Methods, and Results of Metrological Investigations of Sensors. *Oceanology*, 58(5), pp. 661-671. doi:10.1134/S0001437018050090
33. Ocherednik, V.V., Zatsepin, A.G., Kuklev, S.B., Baranov, V.I. and Mashura, V.V., 2020. Examples of Approaches to Studying the Temperature Variability of Black Sea Shelf Waters with a Cluster of Temperature Sensor Chains. *Oceanology*, 60(2), pp. 149-160. doi:10.1134/S000143702001018X
34. Podymov, O.I. and Zatsepin, A.G., 2016. Seasonal Anomalies of Water Salinity in the Gelendzhik Region of the Black Sea according to Shipborne Monitoring Data. *Oceanology*, 56(3), pp. 342-354. doi:10.1134/S0001437016020156
35. Zatsepin, A.G., Piotouh, V.B., Korzh, A.O., Kukleva, O.N. and Soloviev, D.M., 2012. Variability of Currents in the Coastal Zone of the Black Sea from Long-Term Measurements with a Bottom Mounted ADCP. *Oceanology*, 52(5), pp. 579-592. doi:10.1134/S0001437012050177

About the authors:

Vladimir V. Ocherednik, Research Associate, Shirshov Institute of Oceanology, Russian Academy of Sciences (36 Nahimovskiy Prospekt, Moscow, 117997, Russia), **SPIN-code: 6522-7608**, **ORCID ID: 0000-0002-3593-7114**, **ResearcherID: G-2850-2017**, **Scopus Author ID: 56520226300**, v.ocherednik@ocean.ru

Andrey G. Zatsepin, Chief Research Associate, Shirshov Institute of Oceanology, Russian Academy of Sciences (36 Nahimovskiy Prospekt, Moscow, 117997, Russia), Dr.Sci. (Phys.&Math.), **SPIN-code: 1707-3104**, **ORCID ID: 0000-0002-5527-5234**, **ResearcherID: E-4999-2014**, **Scopus Author ID: 7004260979**, zatsepin@ocean.ru

Contribution of the co-authors:

Vladimir V. Ocherednik – manufacturing and programming of the thermoresistor chains; thermoresistor chain approbation, calibration and installation on the shelf; carrying out research, in particular the experiments; data collection, processing, analysis and interpretation of the obtained data; software development; constructing images and writing the paper text; acceptance of responsibility for all aspects of the work, integrity of all parts of the paper and its final version

Andrey G. Zatsepin – data analysis; idea formation; formulation of key aims and objectives; consultation and assistance in writing the paper text; acceptance of responsibility for all aspects of the work, integrity of all parts of the paper and its final version

The authors have read and approved the final manuscript.

The authors declare that they have no conflict of interest.